JOURNAL OF INFORMATION AND COMMUNICATION TECHNOLOGY
https://e-journal.uum.edu.my/index.php/jict

How to cite this article:
Mohd Sharif, N. A., Harun, N. H., & Yusof, Y. (2024). Colour image enhancement model of retinal fundus image for diabetic retinopathy recognition. *Journal of Information and Communication Technology, 23*(2), 293-334. https://doi.org/10.32890/jict2024.23.2.5

Colour Image Enhancement Model of Retinal Fundus Image for Diabetic Retinopathy Recognition

[1]Nurul Atikah Mohd Sharif, [2]Nor Hazlyna Harun
& [3]Yuhanis Yusof
Data Science Research Lab, School of Computing,
Universiti Utara Malaysia, Malaysia

[*1]nurulatikahmohdsharif91@gmail.com
[2]hazlyna@uum.edu.my
[3]yuhanis@uum.edu.my
*Corresponding author

Received: 25/3/2024 Revised: 17/3/2024 Accepted: 23/4/2024 Published: 30/4/2024

ABSTRACT

Diabetic retinopathy (DR) features are typically identified through ophthalmologist eye examinations, but these images often face challenges like low contrast, non-uniform illumination, and colour inconsistency, affecting the diagnosis accuracy. Therefore, this study introduces two novel techniques to improve image quality. One is applying colour image processing techniques to original retinal fundus images, overcoming existing algorithm limitations. Firstly, a new colour correction algorithm was proposed based on Tuned Brightness Controlled Single-Scale Retinex (TBCSSR) named Fuzzy TBCSSR Histogram Matching (*f*TBCSSR*hm*) to address the issue

of colour inconsistency in the dataset. Secondly, based on hybrid particle swarm optimisation-contrast stretch (HPSOCS), the hybrid of TBCSSR and HPSOCS named *e*TBCSSR-HPSOCS algorithm is introduced to tackle the limitations of the standard Particle Swarm Optimisation (PSO) algorithm in HPSOCS, which is prone to local optima and exhibits low convergence rates. This technique combines the L-component of the LAB colour model with an enhanced velocity mechanism in PSO and contrast stretching (*lav*HPSOCS). Its goal is to fine-tune parameters automatically, reduce over-enhancement, avoid unwanted artefacts, and preserve intricate details. This approach improves optimisation by balancing exploration and exploitation and refining velocity control. The proposed algorithm underwent both qualitative and quantitative evaluations. Tests on 100 retinal fundus images from primary datasets were performed to benchmark the algorithm against three existing approaches. The results show that the qualitative performance of the proposed enhancement is more favourable to ophthalmologist specialists than other images. Quantitatively, *e*TBCSSR-HPSOCS outperforms others with the lowest mean squared error (MSE) of 42.72859, the highest peak signal-to-noise ratio (PSNR) of 32.768, and entropy of 0.977.

Keywords: Image colour processing, Image enhancement, Optimisation, Retinal fundus image.

INTRODUCTION

Diabetic retinopathy (DR) is a condition characterised by blood vessel damage in the retina due to long diabetes duration, uncontrolled diabetes, and older age (Magliah et al., 2018). It is the earliest complication sign and is often overlooked when other microvascular abnormalities are not recognised (Chew et al., 2018; Solomon et al., 2017). Malaysia enforces an annual eye screening routine for diabetic patients to detect asymptomatic DR severity (Ministry of Health Malaysia, 2015; Rashid, 2023). Morphological features (MF) criteria, such as colour, shape, size, and texture, are crucial for early screening assessment and DR staging (Colomer et al., 2020; Panwar et al., 2020). Finding the critical component of MF criteria in determining and understanding DR features is significant in helping in early screening assessment and DR staging (Lechner et al., 2017). The critical criteria component will help the grader trainer classify the

severity of DR based on the abnormal features of the retinal fundus image. Digital image processing, which includes image acquisition, enhancement, restoration, colour processing, wavelets and multiresolution processing, compression, morphological processing, segmentation, representation and description, and recognition, can improve the quality of fundus images (Gonzalez & Woods, 2017). Two approaches to improve retinal fundus image quality are adjusting colour inconsistency and enhancing contrast and illumination to enable MF visibility and recognition (Cao & Li, 2020).

This research aims to determine the required features for diabetic retinopathy screening (DRS) by analysing the critical morphological features used by medical practitioners. Four categories of morphological features on retinal fundus images are defined through literature findings: colour, shape, size, and texture. However, not all four features are compulsory for examination during DRS (Colomer et al., 2020; DeMarco et al., 2018). This difference in practice and theory indicates that without standard features, it can interfere with determining critical information, prognosis, treatment planning, and the appropriate image processing algorithm (Kim et al., 2020). Retinal fundus image datasets come in various sizes and colours, and colour image processing is widely used in medical images. Enhancement of the dominant colour channel within the standard colour of retinal fundus images can affect screening, diagnosis, and treatment efficiency (Badano et al., 2015; Raj & Martini, 2019). Tuned Brightness Controlled Single-Scale Retinex (TBCSSR) is one of the recent advances of the Retinex technique, developed on the basic Single-Scale Retinex (SSR) where TBCSSR that can enhance colour images while preserving their standard brightness and natural appearance (Al-Ameen & Sulong, 2015).

Various image enhancement techniques have evolved over the years, including contrast stretching (CS) (Al-amri et al., 2010), histogram equalisation (HE) (Gonzalez & Woods, 2008), image negative (IN) (Swamy & Sakkara, 2017), brightness enhancement (BE) (Mohammed et al., 2013), gray-level slicing (GL) (Dabass & Vig, 2018), and CLAHE (Bhatia & Kumar Rawat, 2018). CS is a popular technique for medical image enhancement due to its ability to improve contrast without altering histogram shape and enhance the visibility of details and features (Cao & Li, 2020; Kaur & Choudhary, 2012; Mohanapriya & Kalaavathi, 2014). However, CS has drawbacks such as loss of

information, colour variation, and colour distortion that may affect human perception. Even though there are other studies proposed as CS alternatives, such as Dhal et al. (2019) utilised Fuzzy Entropic Bi-Histogram Fuzzy Contrast Stretching (FEBHFCS) and Preethi and Maheswari (2019) utilised Bare-Bones Particle Swarm Optimization on CS. However, this study selects a proposed Hybrid Particle Swarm Optimization - Contrast Stretching (HPSOCS) to be improvised as it can segment the region of interest based on the bright and dark area and conduct CS on the segmented area.

However, the limitations due to the implementation of the S-component of the hue, saturation, intensity (HSI) colour model and standard PSO implementation in HPSOCS may produce over or under-saturation of white light towards natural colour and a low convergence rate in iteration (Harun et al., 2020; Li et al., 2007; Sousa-ferreira & Sousa, 2017). Sousa-ferreira and Sousa (2017) mentioned that the exploration-exploitation trade-off determines efficient and accurate optimisation and controls the standard velocity update. Therefore, alternative colour conversion is needed to be converted to a prominent region of interest in the retinal fundus image, and integrating with the information obtained by the velocity equation through the velocity limitation range can give a different best solution (Sousa-ferreira & Sousa, 2017). This study comprises six topics: the introduction, related work, methodology, design and development, result and evaluation, and conclusion and future work.

RELATED WORK

Digital image processing involves manipulating images to obtain desired outputs, extracting attributes, and recognising individual objects. Gonzalez and Woods (2017) provide an overview of digital image processing fundamentals (Figure 1), including image acquisition, filtering and enhancement, colour image processing, segmentation, and pattern classification. This research includes morphological feature identification, image colour processing, and image classification. The image colour processing model proposed (Figure 2) includes colour correction, colour conversion, segmentation, and enhancement.

Figure 1

Methodologies Applied to Images. Adopted From Gonzalez and Woods (2017)

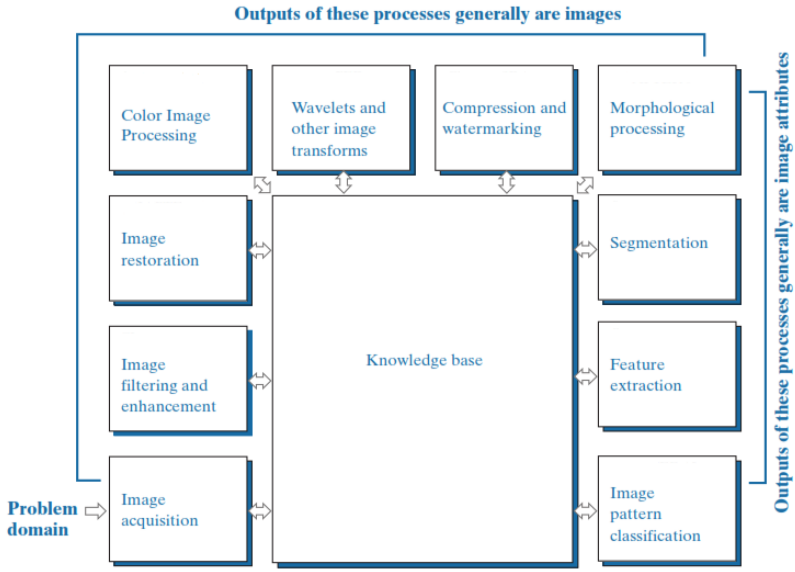

Figure 2

Proposed Image Colour Processing Model

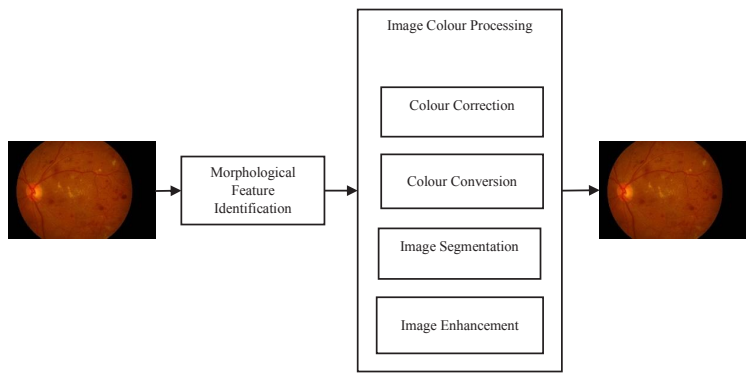

Morphological Feature Identification

Morphology, derived from the Greek word "morphology," refers to studying the structure and form of animals and plants. It is crucial

for image understanding and identification, prognosis, and treatment planning in the medical field. Morphological features are divided according to the type of image data used, such as blood smear images, hematoxylins and eosin (H&E) stained images, pap smear images, computed tomography (CT) images, cell images, and fundus images. Six morphological features can be deployed in image processing for medical image datasets: shape, texture, colour, size, intensity, and geometrical (Batchelor, 2012; Elloumi et al., 2019; Hegde et al., 2019; Kumar & Prateek, 2020; Lin et al., 2019; Wei et al., 2019). Shape is an object's visual representation from Kendall (1984), while texture refers to the visual-tactile quality of its surface (Shapiro, 2001). Colour features include colour space, distribution, histogram, intensity, contrast, and composition (Jyotismita Chaki, 2021).

In medical images, size is a critical feature characteristic with significant diagnostic and analytical value. Size is often considered and utilised in various contexts, such as tumour size, organ size, pathological features, anatomical measurements, and region of interest (ROI) size (Cai et al., 2023; Larici et al., 2017; Yasui et al., 2019). Intensity refers to the brightness or luminance of pixels within the image, often correlated with the grayscale value of each pixel. High-intensity areas are brighter, while low-intensity areas are darker. Adjusting the intensity of an image can involve techniques like contrast enhancement (CE), histogram equalisation, or applying filters to highlight specific features or details (Paulus & Hornegger, 1995). Understanding and determining the criteria of morphological features discussed in this topic will help researchers define the morphological feature that will be finalised for further process. Morphological features are essential for understanding and identifying the characteristics of an image, which are crucial for prognosis and treatment planning in the medical field.

Colour Image Processing

Colour image processing involves manipulating digital images containing colour information, typically consisting of three channels: Red, Green, and Blue (RGB). Techniques in colour image processing include colour correction, enhancement, segmentation, object detection, and classification (Gonzalez & Woods, 2017). Common techniques include colour space conversion, which converts between different colour representations like RGB, CMYK, HSV, and Lab (Ibraheem et al., 2012). Colour correction adjusts colours to compensate for lighting conditions, white balance, or other factors,

making the image more visually appealing or accurate (Fang, 2021). Enhancements improve visual quality or highlight specific features (Kumar Vishwakarma & Mishra, 2012). Segmentation partitions an image into regions based on colour information for object detection or image analysis (Garcia-Lamont et al., 2018). Feature extraction extracts relevant features from colour images for pattern recognition or machine learning (Tian, 2013). Colour-based object detection and tracking identify and track objects in images based on their colour properties (Deshpande & Emmanuel, 2016). Colour image filtering applies filters or transformations to achieve desired effects or remove noise (Rastislav Lukac & Plataniotis, 2011).

Colour inconsistency is an issue in retinal fundus images that needs to be handled. Pai (2019) compared three colour normalisation techniques: White patch Retinex technique, gamma correction, and histogram matching or specification. The finding indicates that White patch Retinex produces better image output under various lighting conditions. There is also a previous comparison among the Retinex method, Histogram Equalization, Gamma Correction and Homomorphic filtering techniques by Dileep and Sreenivasa Murthy (2011), which found that the Retinex method of colour image enhancement gives more contrast-enhanced results without destroying any parts of the image that does not require enhancement. Aris et al. (2021) also compare six types of colour constancy algorithms, namely, gray world (GW), white patch (WP), modified white patch (MWP), progressive hybrid (PH), shades of gray (SoG) and gray edge (GE) applied on thick and thin smear malaria images. The results indicate that the SoG algorithm resultant image has proven to be the best colour constancy algorithm, where white patches become the closed resultant image. Out of various comparison studies, the Retinex technique was the best for exploring the solution for retinal fundus image colour inconsistency.

The Retinex technique, introduced by Edwin Land in 1964, is based on the human colour vision process, which consists of the retina and cortex (Land, 1964). It aims to explain human colour constancy by calculating lightness sensations in each channel. A review by Hussein et al. (2019) summarised numerous Retinex techniques that evolved from the original Retinex technique. Table 1 shows the various Retinex techniques based on each technique's criteria. Instead of the various techniques that evolved from the original Retinex, the most common adaptive Retinex technique developed through it is Single-scale Retinex (SSR) proposed by Jobson et al. (1997).

Table 1

Various Retinex Techniques With Its Criteria. Adopted from Hussein et al. (2019)

Techniques	Recursive matrix	Path Geometry	Fast	Real time application	Center surround	Appearance	Dynamic range	Enhancement of 8 bit colour	"Halo effect"	Random Walks
Path based algorithm	/	X	/	/	/	/	/	/	/	X
Recursive algorithm	X	/	/	/	/	/	/	/	/	X
Random Spray Retinex (RSR)	/	/	X	X	/	/	/	/	/	/
Single Scale Retinex (SSR)	/	/	/	/	X	X	X	/	/	/
Multi Scale Retinex (MSR)	/	/	/	X	X	X	X	/	/	/
Multi Scale Colour Restoration (MSRCR)	/	/	/	/	X	X	/	X	/	/
Multi Scale Retines with Initial Approximation (MSRIA)	/	/	/	/	X	X	/	/	/	
Multi Scale Retinex with Wide Dynamic Range (MSRWDR)	/		/	/	X	/	/	/	X	/
Retinex Based Adaptive Filter (RAF)	/	/	/	/	X	/	/	/	X	/
Fast Multi Scale Retinex (FMSR)	/	/	X	/	X	/	/	/	X	/

/-denotes the technique exhibits the selected criteria

X- denotes the technique does not exhibit the selected criteria

SSR technique has evolved to meet specific criteria for various applications, with a recent advance of the Retinex technique being tuned brightness-controlled single-scale Retinex (TBCSSR), which was developed on the basic Single-scale Retinex (SSR) technique (Al-Ameen & Sulong, 2015). TBCSSR can achieve artefact-free, fast implementation, low computation cost, acceptable visual quality, and improved contrast while maintaining standard brightness and natural appearance. The mathematical equation of TBCSSR has been improved by replacing 2σ with $M \times N$ and adding a tuning parameter for brightness control by Al-Ameen and Sulong (2015). The ameliorated sigmoid function is combined with the standard sigmoid function, and the final process to produce the contrast-adjusted image with an expansion of dynamic range is computed using a normalisation procedure. The TBCSSR technique has been improvised by Al-Ameen and Sulong (2015) to improve image illumination and colour consistency, but it only works on grayscale images with one colour channel that contains intensity information without wavelength. It can lead to biased and inconsistent models. Hussein et al. (2019) suggested designing a model that is less dependent on the optimisation parameter and focusing on measurable metrics related to image degradation level to address this issue.

As discussed above, where the need to cater for the manual setting of the parameter in TBCSSR and colour matching, hence, fuzzy rule-based technique and histogram matching or histogram specification are among the standard technique practices by researchers, respectively (Grundland & Dodgson, 2007; Kagarlitsky et al., 2009; Xiao et al., 2018). There are discussions on techniques that can automate the parameter setting, as Huang et al. (2020) surveyed, where automatic parameter tuning is classified into three approaches based on metaheuristic techniques. In contrast, a discussion of colour image-matching techniques has been presented in detail by Faridul et al. (2016). A comprehensive overview matching technique offers the following: From the literature findings, the fuzzy rule-based technique and statistical colour mapping techniques can be explored to address this study's problem.

Fuzzy regression analysis evaluates the functional relationship between dependent and independent variables and identifies the best-fit model for characterising the relationship (Shapira et al., 2013). Histogram specification is considered the best normalisation

technique, as it allows for robust utilisation of colour information in classification and increases separation across lesion-type clusters in chromaticity space (Gonzalez & Woods, 2017). In summary, the integration of the Retinex, colour matching, and fuzzy techniques can be considered in this research due to its ability to help solve colour correction issues in the pre-processing stages in image processing.

CE is crucial for enhancing image quality by improving contrast, edge increment, and noise decline. Modern techniques in medical imaging include histogram equalisation (Singh et al., 2019), contrast stretching (Al-amri et al., 2011), image negative (Deepak et al., 2012), low light image (Gu et al., 2018), and gray level slicing (Sarangi et al., 2014). Recent advances in CE, such as Adaptive Histogram Equalization, Contrast-Limited Adaptive Histogram Equalization (CLAHE) (Ratanapakorn et al., 2019; Sharif & Shah, 2019), and Top-Hat Transformation (Bhateja et al., 2019), are widely used to enhance retinal fundus images. These techniques have evolved from conventional to modern techniques in the medical field. Low-contrast photographs can be caused by nonlinearity, inadequate illumination, or the imaging sensor's limited dynamic range. To improve image analysis processes, deepening the contrast of images is essential (Fathy et al., 2018). Contrast Stretching (CS) is a traditional image CE technique based on global histogram techniques. It extends the range of intensity values of a picture to encompass the entire dynamic range of an image and works best with low-contrast images.

The enhancement-based technique (CE) is being improved to improve efficiency but is limited in accuracy and optimisation due to its limitations on specific image spots (Qureshi et al., 2019; Yadav et al., 2017). Optimisation is choosing the best element from a set of alternatives to provide the best possible decision in a given set of constraints (Burke & Kendall, 2014). Recent research has integrated various optimisation techniques with image enhancement techniques, such as classical CE with Particle Swarm Optimization (PSO) (Zakwan et al., 2019), Genetic Technique (Çam et al., 2018), and a hybrid of Cuckoo Search Optimization with PSO (Chandrashekar & Sreedevi, 2020). PSO is a widely used optimisation technique for image enhancement, with its speed and low memory requirements making it effective in various applications such as signal processing, neural networks, electrical power, and data mining (Paul et al., 2019; Subramanya Jois et al., 2019). However, objective functions must

compromise between global and local information to achieve good results in image enhancement.

A technique proposed by Harun et al. (2020) combines contrast stretching and PSO techniques to optimise segmentation processes for the region of interest (ROI) and enhance white blood cell (WBC) images. HPSOCS converts RGB colour models to HSI colour models, selecting the S-component of the WBC image as input for segmentation optimisation. The optimisation process starts with converting RGB colour models to HSI colour models, and the fitness function for the optimisation is based on the S-component of the WBC image. The HPSOCS algorithm has two main concerns: over or under saturation of white light towards natural colours and the implementation of standard PSO algorithm in HPSOCS, resulting in a low convergence rate in iteration. The standard velocity update must consider and control exploration-exploitation trade-offs to achieve efficient and accurate optimisation (Sousa-ferreira & Sousa, 2017). Therefore, alternative colour conversion techniques should be integrated with the information obtained by the velocity equation through the velocity limitation range to provide a different best solution.

Limiting velocity in PSO is a common technique used to prevent particles from moving too quickly through the search space, improving the stability and convergence properties of the algorithm (Barrera et al., 2016). Unbounded velocities can lead to erratic behaviour or overshooting of the optimum solution. There are various ways to impose velocity limitations in PSO, such as velocity clamping, coefficient adjustments, dynamic inertia weight, normalisation, and adaptive mechanisms. By employing one or a combination of these techniques, practitioners can effectively control and limit the velocities of particles in PSO, promoting smoother convergence and better exploration-exploitation balance. The choice of technique depends on the specific characteristics of the optimisation problem and the desired behaviour of the algorithm.

METHODOLOGY

Research design is a storyline of the whole research to accomplish the objectives. Figure 3 visualises the overall process of this research. This research has four main phases: data collection and preparation, model design, model development and model evaluation.

Figure 3

Research Design of the Proposed Model

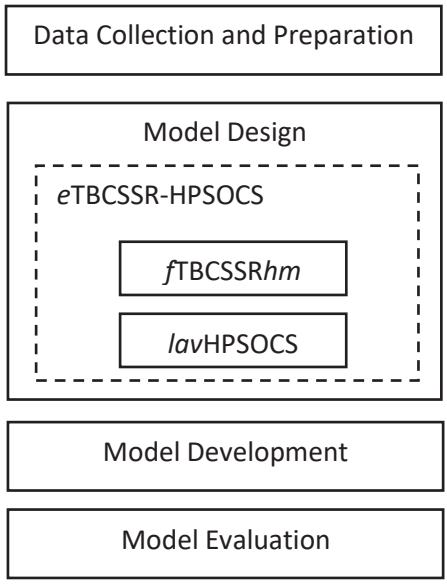

Data Collection and Preparation

The data used in this research is a primary data source that includes information collected and processed directly by the researcher, such as observations, surveys, interviews, and focus groups. This research's primary data focuses on the retinal fundus image collected and processed by the Ophthalmology Clinic, Hospital Universiti Sains Malaysia (HUSM). The image was captured using a non-mydriatic fundus camera. The criteria for the original retinal fundus image are as follows:

- Image type: JPG file
- Image dimension: 3008 x 2000 pixels
- Image size: less than 1 MB each picture
- Image resolution: 96 x 96 dpi
- Bit depth: 24 bits

One hundred retinal fundus images are collected and named sample images. Out of 100 images, 30 retinal fundus images were chosen by ophthalmologists as the best and preferred colour retinal fundus

image. This image is used as a standard colour image and provides a set of reference images for colour correction purposes as a reference image.

Model Design and Development

Model design involves morphological features, colour correction, and image enhancement with an optimisation algorithm. In the first stages, for morphological features, Elloumi et al. (2019), Guo (2020), and Martins et al. (2020) identified size, shape, and colour as the main morphological features for retinal fundus images, which have been discussed with ophthalmologists and have been set as three main features to be focused throughout this research. For colour correction, a new colour correction algorithm is proposed, namely Fuzzy Tuned Brightness Controlled Single-Scale Retinex Histogram Matching (fTBCSSRhm) technique, which integrates the Fuzzy Rule-based and TBCSSR on a green colour channel. TBCSSR is calculated using Gaussian Surround Function (GSF) (Equation 1 and Equation 2), Single-scale Retinex (SSR) (Equation 3) and modified sigmoid function (Equation 4 until Equation 7). It is then integrated with histogram matching or histogram specification algorithm. The fuzzy rule-based model is built using MATLAB and used to determine the β value in the TBCSSR algorithm. The algorithm then matches the histogram using a reference image as a standard colour retinal fundus image. The output is images with the same colour as the ophthalmologist's preferred colour.

1. Compute modified Gaussian Surround Function (GSF) using Equation 1 and Equation 2:

$$G(x,y) = \frac{K \times e^{-\frac{(A^2+B^2)}{2(M\times N)^2}}}{\beta} \tag{1}$$

$$K = \frac{1}{\sum_{i=1}^{M}\sum_{j=1}^{N} e^{-\frac{(A^2+B^2)}{2M\times N^2}}} \tag{2}$$

2. Compute the Single-scale Retinex (SSR) using Equation 3:

$$O_{SSR}(x,y) = \log[L(x,y)] - \log[G(x,y) \otimes L(x,y)] \tag{3}$$

$O_{SSR}(x, y)$ refers to SSR output, $L(x, y)$ refers to low-contrast images and $\otimes$ refers the convolution process. Improvement on the GSF equation by following points: First, replacement of 2σ by M×N that represents the image dimensions; Second, addition of β as tuning parameter for brightness control with fulfils $\beta > 0$, otherwise for $\beta \geq 2$, the modified sigmoid function is implemented. The standard sigmoid function is as in Equation 4:

$$f(g) = \frac{1}{1 + e^{-\alpha(g)}} \tag{4}$$

Modification of standard sigmoid function is on the α value and ameliorated version of the latter by default adjusting constant, $\gamma = 2$. Equation 5 for α as follows where T as regulating value by default equal to 2:

$$\alpha = 1 + (\beta - T) \tag{5}$$

Hence, the ameliorated sigmoid function is combined as in Equation 6:

$$s(g) = \frac{1}{1 + e^{-(1+(\beta-T))\times(g-\gamma)}} \tag{6}$$

The final process to produce the contrast-adjusted image, $s(g)$ with the expansion of the dynamic range to fit its full natural interval by computing a normalisation procedure using Equation 7:

$$n(s) = \frac{[s(g) - min(s(g))]}{[max(s(g)) - min(s(g))]} \tag{7}$$

The $n(s)$ represents the normalised image, and min and max are employed as the minimum and maximum pixel values of the $s(g)$.

Hybrid PSO-Contrast stretching (HPSOCS) for retinal fundus images is improved for image enhancement optimisation. HPSOCS segmentises the bright and dark regions of interest, enhancing the image. However, it selects the S-component as input information, leading to over or under-saturation white light. The input information is replaced with the L-component of the LAB colour model to maintain the standard colour mapping through colour correction. The study also

proposes improvements to the standard PSO algorithm by adjusting the velocity initialisation of the lightness component and velocity limitation, which can control exploration or exploitation tendencies in the particle searching space. The new image enhancement optimisation is called Lightness Adjusted Velocity of Hybrid Particle Swarm Optimization Contrast Stretching (*lav*HPSOCS).

Model Evaluation

Model evaluation is a performance evaluation process that involves two types: model validation and model verification. Validation ensures the output meets user needs, like an ophthalmologist in this research, while verification ensures the model performs better or matches literature models. The model validation process involves two sections based on the image and algorithm, with discussions between an ophthalmologist and a researcher. Model verification is performed by evaluating the enhanced image qualitatively and quantitatively. For qualitative analysis, the appointed ophthalmologist was requested to conduct subjective analysis by grading the quality of the enhanced images. For quantitative analysis, two approaches are used, which are based on statistical performance matrixes and comparing among several state-of-the-art ones. Statistical performance matrixes include Mean Squared Error (MSE), Peak Signals to Noise (PSNR), Structural Similarity Index Metric (SSIM), Universal Quality Index (UQI) and Image Entropy. The detailed discussion related to the statistical evaluation as quantitative evaluation is presented in Equation 8 until Equation 12.

Mean Squared Error (MSE) is defined as follows:

$$MSE = \frac{1}{MN}\sum_{n=1}^{M}\sum_{m=1}^{N}[\hat{g}(n,m) - g(n,m)]^2 \tag{8}$$

PSNR is defined as follows:

$$PSNR = -10\log_{10}\frac{MSE}{S^2} \tag{9}$$

Where,

S is the maximum pixel value.

SSIM is defined:

$$SSSIM(x,y) = \frac{(2\mu_x + c_1)(2\sigma_{xy}c_2)}{(\mu_x^2 + \mu_y^2 + c_1)(\sigma_x^2 + \sigma_y^2 + c_2)} \quad (10)$$

Where,
μ_x the average of x; μ_y the average of y; σ_x^2 the variance of x; σ_y^2 the variance of y; σ_{xy} the average of x and y; $c_1 = (k_1 L)^2, c_2 = (k_2 L)^2$ two variables to stabilise the division with a weak denominator; L the dynamic range of the pixel-value; $k_1 = 0.01$ and $k_2 = 0.03$ by default.

UQI is as follows:

$$Q(x,y) = \frac{4\sigma_{xy}\bar{x}\bar{y}}{(\sigma_x^2 + \sigma_x^2)[(\bar{x})^2 + (\bar{y})^2]} \quad (11)$$

entropy is:

$$entropy = -\sum_i P_i \log_2 P_i \quad (12)$$

Where,
P_i is the probability that the difference between 2 adjacent pixels is equal to i

DESIGN AND DEVELOPMENT

This research focuses on three main features in determining the classification of the diabetic retinopathy phase: size, shape, and colour. The literature review reveals that these three features are crucial for ophthalmologists to determine the severity and stage of diabetic retinopathy and different types of diagnosis, such as diabetic macular oedema. The size and shape of abnormalities on the retinal fundus image, such as microaneurysms and haemorrhage, help determine the severity and stage of diabetic retinopathy. The shape and colour of the retinal fundus image also help determine abnormalities like cotton wool spots and hard exudate, as each abnormality is treated differently. It is recommended that the image be improved without significant changes to these three features to avoid false diagnoses if any changes occur during the processing of the original image.

The TBCSSR algorithm's performance relies heavily on the β value parameter, which depends on the image size. This study proposes

integrating TBCSSR with a fuzzy rule-based model, resulting in the Fuzzy Tuned Brightness Controlled Single-Scale Retinex (*f*TBCSSR). The *f*TBCSSR is then integrated with a histogram matching algorithm, the Fuzzy Tuned Brightness Controlled Single-Scale Retinex Histogram Matching (*f*TBCSSR*hm*), to ensure the image complies with the standard colour histogram of the retinal fundus image. The fuzzy rule-based model includes an input variable, fuzzy knowledge base, inference engine, working memory, and output of the β parameter. The model is built using MATLAB's fuzzy logic toolbox. The component of fuzzy ruled-based model integration is shown in Figure 4, and the range of fuzzy set values for input and output variables is presented in Table 2.

Histogram colour matching involves comparing the retinal fundus image's histogram with a standard reference histogram from 30 reference retinal images. These images are chosen by specialist ophthalmologists based on the recommended colour of the fundus image. As the standard reference histogram was obtained, the process of histogram colour matching continued by mapping each colour channel from the original retinal fundus image with the standard colour channel value using cumulative distribution function (CDF) (Equation 13). The complete Colour Correction algorithm known as *f*TBCSSR*hm* is presented as Algorithm 1, where the highlighted step is the proposed technique.

$$F(x) = \int_{-\infty}^{x} \frac{1}{\sqrt{2\pi\sigma}} exp\left[-\frac{(t-\mu)^2}{2\sigma^2}\right] dt, \sigma > 0 \qquad (13)$$

where, is mean, is variance and is standard deviation.

Figure 4

The Component of Fuzzy Rule-Based Model Integration.

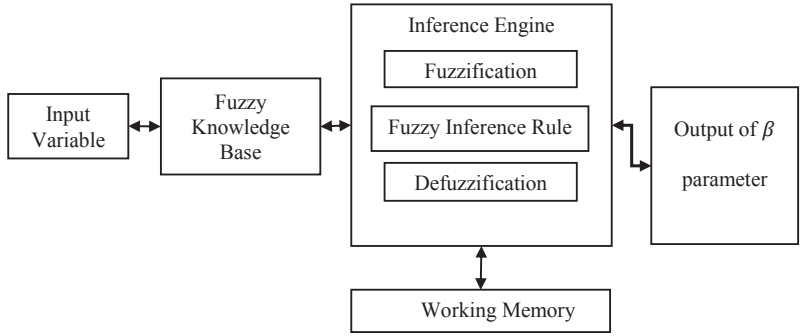

Table 2

Range of Fuzzy Set Value and Its Linguistic Variable for Input and Output

	Variable	Fuzzy Interval	Set	Linguistic Value	Fuzzy Interval	Type MF	Parameters
Input	M	0 - 5000		Small	0-2000	Triangle	[0 0 2000]
				Medium	1500 - 2500	Triangle	[1500 2000 2500]
				Large	2000 - 5000	Trapezoidal	[2000 3000 5000 5000]
	N	0 - 5000		Small	0-2000	Triangle	[0 0 2000]
				Medium	1500 - 2500	Triangle	[1500 2000 2500]
				Large	2000 - 5000	Trapezoidal	[2000 3000 5000 5000]
Output	β	0 - 10		Low	0-3	Trapezoidal	[0 4 5]
				Medium	4-8	Triangle	[4 6 8]
				High	7-10	Trapezoidal	[7 8 10]

Algorithm 1. fTBCSSRhm Algorithm (Colour Correction)

1. **Input**: a: original images, d: standard histogram of reference images
2. **for** each a
3. compute fuzzy rule-based model to find parameter
4. compute TBCSSR formula with input parameter (Equation 1 until Equation 7)
5. map histogram with d using equation 6
6. **end for**
7. **Output**: corrected colour of resultant image

The study by Harun et al. (2020) proposes a hybrid Particle Swarm Optimisation Contrast Stretching (HPSOCS) algorithm to improve the segmentation of dark and bright regions of interest in retinal fundus images. HPSOCS uses the colour conversion of RGB to HSI, with the S-component of HSI used as input for a standard PSO algorithm. However, due to the weakness of the S-component of HSI and the standard PSO algorithm, this study proposes an alternative colour conversion using the L-component of LAB and a limitation on the velocity component of PSO called Lightness Adjusted Velocity of Hybrid Particle Swarm Optimization Contrast Stretching (*lav*HPSOCS).

The original retinal fundus image is converted into a LAB colour channel, influencing particles' initialisation and subsequent behaviour in the PSO algorithm. In this modified approach, an additional factor called "lightness" is introduced for each particle, which influences its initial velocity and for the main loop in each iteration through the velocity limitation range and position limitation range. Two proposed velocity adjustments are made during initialisation and in the main PSO loop for each iteration.

The first adjustment is on the velocity initialisation, where the standard velocity initialisation with the rand (range) is denoted as a random value chosen uniformly from the specified range. The second adjustment is for the PSO main loop, where the new velocity limit is determined using Equations 14-16. By adjusting the velocity limit, particles navigate the search space for optimal solutions, allowing exploration and exploitation. Balancing between exploration and exploitation is crucial for the PSO algorithm to converge towards good solutions efficiently.

solutions efficiently.

$$Vel_{new} = \min(max(V_{old}, VelMin), VelMax) \quad (14)$$

$$VelMax = 0.1(\max\_\text{lightness} - min\_lightness) \quad (15)$$

$$VelMin = -VelMin \quad (16)$$

The performance of *lav*HPSOCS algorithm produces six types of bright and dark segmented retinal fundus images based on the lightness of the images. One bright and one dark segmented image is selected for local contrast stretching, and the enhanced bright and dark spot image is combined and converted into RGB colour channels as required by specialist ophthalmologists' preferences. The complete algorithm for *lav*HPSOCS is presented in Algorithm 2 (the highlighted step is the proposed technique), while the parameter for the PSO is presented in Table 3.

Algorithm 2. **Lightness-Adjusted Velocity HPSOCS (*lav*HPSOCS) Algorithm**

Input:

O_{RGB} – Original Image with RGB colour model
P – Swarm size population
D – Image with L-component of O_{LAB} as input dimension
T – Maximum iteration
LB – Lower bound
UB – Upper bound
F – Fitness function

Output:

$gbest$ – the best position found
S_{RGB} – Segmentise image
I_{RGB} – Improved image

1. Start
2. Convert O_{RGB} to O_{HSI} colour model
3. Initialise X_i randomly within [LB, UB]^D
4. Initialise $V_i^{new\_t}$
5. Evaluate the fitness $f(X_i)$
6. Initialise $pbest_i$ with a copy of X_i
7. Initialise $gbest$ with a copy of X_i with the best fitness
8. For each iteration until T, maximum iteration:
9. For each particle i in a swarm population size P
10. For each data vector, z_p

(continued)

Algorithm 2. **Lightness-Adjusted Velocity HPSOCS (*lav*HPSOCS) Algorithm**

11. Update V_i
12. Calculate Euclidean distance
13. Evaluate the fitness $f(X_i^t)$
14. Update and according to equation **Error! Reference source not found.**14), **Error! Reference source not found.**15) and **Error! Reference source not found.**15)
15. Update $pbest_i \leftarrow X_i^t$ if $f(pbest_i) < f(X_i^t)$
16. Update $gbest \leftarrow X_i^t$ if $f(gbest) < f(X_i^t)$
17. End for
18. End for
19. End for
20. Convert S_I to S_{RGB} colour model
21. Compute Contrast Stretching on S_{RGB}
22. End

Table 3

Parameter Values For PSO Algorithm

Parameter	Value
Number of particles	30
Maximum iteration	6
Inertia weight	1
Inertia Weight Damping Ratio	0.99
Personal Learning Coefficient	1.5
Global Learning Coefficient	2.0

Integration of colour correction (fTBCSSRhm) and image enhancement optimisation (lavHPSOCS) is called *e*TBCSSR-HPSOCS. A full flow of the proposed algorithm is shown in Algorithm 3.

Algorithm 3. **eTBCSSR-HPSOCS Algorithm**

Input:

O_{RGB} – Original Image with RGB colour model
P – Swarm size population
D – Image with L-component of O_{LAB} as input dimension
T – Maximum iteration
LB – Lower bound
UB – Upper bound
F – Fitness function

Output:

$gbest$ – the best position found
S_{RGB} – Segmentise image
I_{RGB} – Improved image

1. Start
2. Convert O_{RGB} to
3. for each O_G colour channel
4. compute fuzzy rule-based model to find β parameter.
5. compute TBCSSR formula with input β parameter (Equation 1 until Equation 7)
6. map histogram with d using equation 6
7. end for
8. Merge $O_{G,new}$ to $O_{RGB,new}$
9. Convert $O_{RGB,new}$ to O_{LAB} colour model
10. Initialise X_i randomly within [LB, UB]^D
11. Initialise $V_i^{new\_t}$
12. Evaluate the fitness $f(X_i)$
13. Initialise $pbest_i$ with a copy of X_i
14. Initialise $gbest$ with a copy of X_i with the best fitness
15. For each iteration until T, maximum iteration:
16. For each particle i in a swarm population size P
17. For each data vector, z_p
18. Update V_i
19. Calculate Euclidean distance
20. Evaluate the fitness $f(X_i^t)$
21. Update $Vel_{new,i}$ and X_{ji}^t according to Equation 7, Equation 8 and Equation 9
22. Update $pbest_i \leftarrow X_i^t$ if $f(pbest_i) < f(X_i^t)$
23. Update $gbest \leftarrow X_i^t$ if $f(gbest) < f(X_i^t)$
24. End for
25. Convert S_I to S_{RGB} colour model
26. Compute Contrast Stretching on S_{RGB}
27. End
28. Result image: I_{RGB}

RESULT AND EVALUATION

A qualitative analysis was conducted using a visual assessment of 20 original retinal fundus images. Table 4 until Table 8 shows 5 out of 20 retinal fundus image assessments focused on three types of features: retinal vessel and retinal haemorrhages, hard exudate, and optic disc. The results showed that both TBCSSR and *f*TBCSSR*hm* produced clear retinal vessels and retinal haemorrhages in all images, as shown in Table 4. However, both produced less-illuminated hard exudate and the optic disc, with some images showing a slightly reddish colour in the centre.

The assessment from Table 4 also indicates that *lav*HPSOCS produces a resultant image with clear features followed by the HPSOCS. At the same time, the contrast stretching technique produced an over-illuminate resultant image on the hard exudate and optic disc. The overall visual assessment focusing on the illumination and image homogenous in Table 6 shows that only the contrast stretching technique produces an over-illuminate resultant with a homogenous image even though no over-illuminate resultant image was assessed on HPSOCS and lavHPSOCS 4 and 13 resultant images out of 20 produced a non-homogenous image from HPSOCS and *lav*HPSOCS respectively. It was followed by the *lav*HPSOCS technique, which produced 20 resultant images with clear retinal vessels and retinal haemorrhage, 11 with clear hard exudate, and 8 with clear optic disc images. The lowest performance of resultant images accessed by the specialist is on the *lav*HPSOCS, where only 19 resultant images accessed as clear retinal vessels and retinal haemorrhage, ten resultant images have clear hard exudate and 13 resultant images with clear optic disc. The balance of resultant images for all techniques contains an over-illumined image section, and some images have no hard exudate.

A score given by a specialist ophthalmologist shown in Table 9 indicates that the *lav*HPSOCS is rated with ‘very good’ for all five questions, which asked about the better resultant image, clarity of features and abnormalities, suitability for DR staging, desired colour representation and no missing criteria. HPSOCS was also rated as ‘very good’ for desired colour representation without missing criteria. The contrast stretching technique was rated ‘bad’ for all questions.

Even though the resultant image looks clearer with pixel distribution normalised and a high dynamic range, it is not accepted from a medical point of view. A specialist ophthalmologist rated *f*TBCSSR*hm* 'very good' in all five questions related to the resultant image, clarity of features and abnormalities, suitability for DR staging, desired colour representation, and missing criteria.

Table 4

First Resultant Retinal Fundus Images Out of 20 Retinal Fundus Images Visual Assessment

	Original Image	TBCSSR	CS	HPSOCS	*f*TBCSSR *hm*	*lav*HPSO CS	*e*TBCSSR-HPSOCS
1		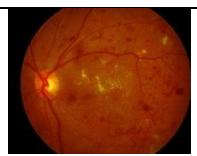 Retinal vessels & retinal haemorrhage: clear Hard exudate: clear Optic disc: clear	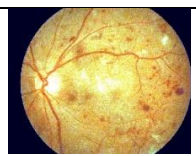 Retinal vessels & retinal haemorrhage: clear Hard exudate: over-illuminated Optic disc: over-illuminated	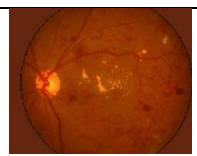 Retinal vessels & retinal haemorrhage: clear Hard exudate: clear Optic disc: clear	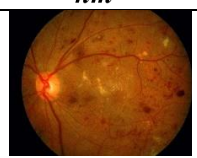 Retinal vessels & retinal haemorrhage: clear Hard exudate: clear Optic disc: clear	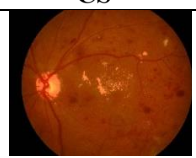 Retinal vessels & retinal haemorrhage: clear Hard exudate: clear Optic disc: clear	 Retinal vessels & retinal haemorrhage: clear Hard exudate: clear Optic disc: clear

Table 5

Second Resultant Retinal Fundus Images out of 20 Retinal Fundus Images Visual Assessment

	Original Image	TBCSSR	CS	HPSOCS	*f*TBCSSR*hm*	*lav*HPSOCS	*e*TBCSSR-HPSOCS
2	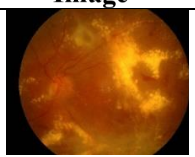	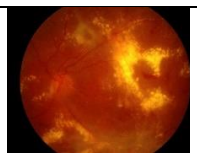	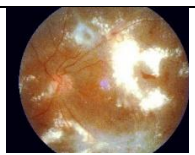	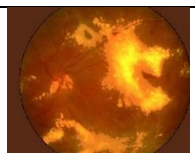	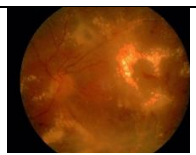	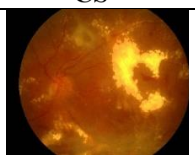	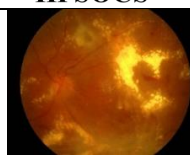
		Retinal vessels & retinal haemorrhage: clear Hard exudate: Clear Optic disc: clear	Retinal vessels & retinal haemorrhage: clear Hard exudate: over-illuminated Optic disc: clear	Retinal vessels & retinal haemorrhage: clear Hard exudate: clear Optic disc: clear Non-homogenous retina	Retinal vessels & retinal haemorrhage: clear Hard exudate: less-illuminated and smaller in size Optic disc: clear	Retinal vessels & retinal haemorrhage: clear Hard exudate: clear Optic disc: clear	Retinal vessels & retinal haemorrhage: clear Hard exudate: slightly over-illuminated Optic disc: clear

Table 6

Third resultant retinal fundus images out of 20 retinal fundus images Visual Assessment

	Original Image	**TBCSSR**	**CS**	**HPSOCS**	***f*TBCSSR*hm***	***lav*HPSOCS**	***e*TBCSSR-HPSOCS**
3	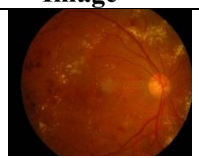	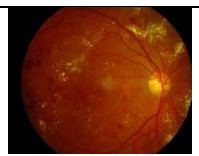	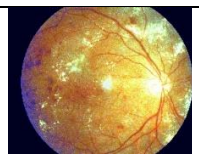	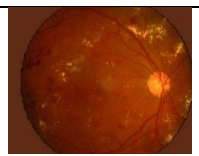	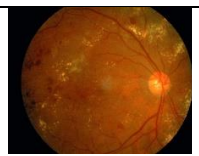	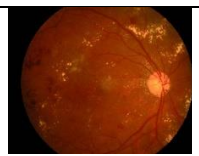	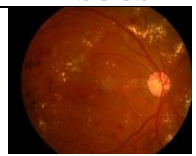
		Retinal vessels & retinal haemorrhage: clear Hard exudate: clear Optic disc: clear	Retinal vessels & retinal haemorrhage: clear Hard exudate: over-illuminated	Retinal vessels & retinal haemorrhage: clear Hard exudate: clear Optic disc: clear	Retinal vessels & retinal haemorrhage: clear Hard exudate: clear Optic disc: clear	Retinal vessels & retinal haemorrhage: clear Hard exudate: clear Optic disc: clear	Retinal vessels & retinal haemorrhage: clear Hard exudate: slightly over-illuminated

Journal of ICT, 23, No. 2 (April) 2024, pp:293-334

Table 7

Fourth Resultant Retinal Fundus Images Out of 20 Retinal Fundus Images Visual Assessment

	Original Image	TBCSSR	CS	HPSOCS	*f*TBCSSR*hm*	*lav*HPSOCS	*e*TBCSSR-HPSOCS
4	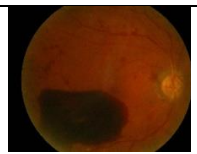	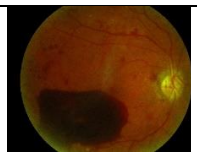	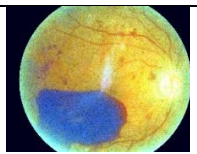	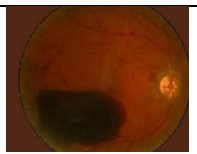	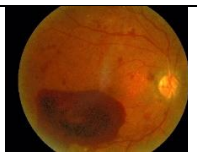	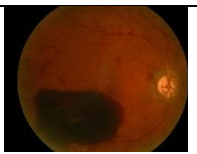	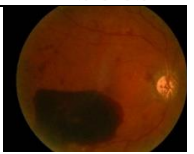
		Retinal vessels & retinal haemorrhage: clear Hard exudate: no hard exudate in this photo	Retinal vessels & retinal haemorrhage: clear Optic disc: over-illuminated	Retinal vessels & retinal haemorrhage: clear Optic disc: clear	Retinal vessels & retinal haemorrhage: clear Hard exudate: no hard exudate in this photo	Retinal vessels & retinal haemorrhage: clear Optic disc: clear	Retinal vessels & retinal haemorrhage: clear Hard exudate: no hard exudate in this photo

Table 8

Fifth Resultant Retinal Fundus Images Out of 20 Retinal Fundus Images Visual Assessment

	Original Image	TBCSSR	CS	HPSOCS	*f*TBCSSR*hm*	*lav*HPSOCS	*e*TBCSSR -HPSOCS
5	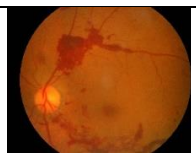	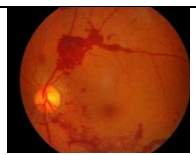	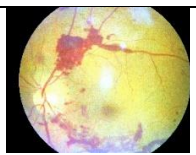		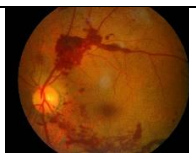	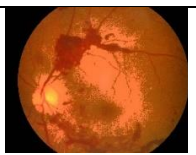	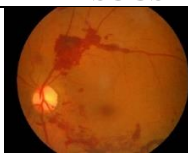
		Retinal vessels & retinal haemorrhage: clear Hard exudate: no hard	Retinal vessels & retinal haemorrhage: clear Optic disc: clear	Retinal vessels & retinal haemorrhage: clear Optic disc: clear	Retinal vessels & retinal haemorrhage: clear Hard exudate: no hard	Retinal vessels & retinal haemorrhage: clear Optic disc: clear	Retinal vessels & retinal haemorrhage: clear Hard exudate: no hard

Table 9

Score For Each Technique Based on the Questions Answered by the Specialist Ophthalmologist. (1 – Very Bad, 2 – Bad, 3 – Neutral, 4 – Good, 5 – Very Good)

No	Questions	TBCSSR	CS	HPSOCS	fTBCSSRhm	lavHPSOCS	eTBCSSR-HPSOCS
	Which algorithm gives a better resultant image?	4	2	4	5	5	4
	Which algorithm enables the abnormalities on the resultant image can be seen clearly?	5	2	4	5	5	4
	Which algorithm provides a suitable resultant image that can be used for DR staging diagnosis?	4	2	4	5	5	4
	Which algorithm produces a resultant image with the desired colour representation?	4	2	5	5	5	4
	Which algorithm produces a resultant image with no missing criteria?	5	2	5	5	5	4

Table 10

Summary of Visual Assessment by Specialist Ophthalmologist on Overall Resultant Retinal Fundus Image

Features	Algorithm	Image Clear	Image Over/less-illuminated
Retinal vessels & retinal haemorrhage	TBCSSR	20	0
	*f*TBCSSR*hm*	20	0
	CS	20	0
	HPSOCS	20	0
	*lav*HPSOCS	20	0
	*e*TBCSSR-HPSOCS	19	1
Hard exudate	TBCSSR	15	2
	*f*TBCSSR*hm*	15	2
	CS	11	9
	HPSOCS	19	0
	*lav*HPSOCS	20	0
	*e*TBCSSR-HPSOCS	10	6
Optic disc	TBCSSR	16	4
	*f*TBCSSR*hm*	16	4
	CS	4	16
	HPSOCS	20	0
	*lav*HPSOCS	20	0
	*e*TBCSSR-HPSOCS	13	7

Despite qualitative analysis results being similar, quantitative analysis reveals that *e*TBCSSR-HPSOCS and *lav*HPSOCS performs better with main evaluation matrices as presented in Table 11. The higher the MSE, PSNR, SSIM and UQI, the better the quality of the image obtained. While, a lower value of entropy produces better image output. The result tabulated in Table 11 indicates that *e*TBCSSR-HPSOCS have better results on the MSE (42.72859), PSNR (32.76795), and entropy (0.97734) compared to other algorithms, while *lav*HPSOCS give better result on SSIM (0.994972) and UQI (0.953187) performance matrices. The result indicates the naturality and colour preference of the *e*TBCSSR-HPSOCS and *lav*HPSOCS resultant image close to the original retinal fundus image. The features are legibly seen, and this technique has also improved the visual perception of the image. This technique can easily identify the areas affected by retinal diseases.

Table 11

Quantitative Assessment on 100 Resultant Images Comparing the Outcome of fTBCSSRhm, lavHPSOCS and eTBCSSR-HPSOCS

Evaluation Matrixes	TBCSSR	CS	HPSOCS	fTBCSSRhm	lavHPSOCS	eTBCSSR-HPSOCS
MSE	91.0455	7901.244	1382.294	291.043537	79.69245	**42.72859**
PSNR	30.22072	9.270211	16.84078	25.4805671	31.29726	**32.76795**
ENTROPY	5.816328	5.241102	6.041048	5.97105761	5.582384	**0.97734**
SSIM	0.965094	0.460441	0.661208	0.85959715	**0.994972**	0.969114
UQI	0.65618	0.340434	0.623577	0.8270516	**0.953187**	3.070121

CONCLUSION AND FUTURE WORK

This research aims to enhance retinal fundus images and reduce constraints related to low quality and human error. Three objectives are set: First, to standardise the colour of retinal fundus images, as colour is crucial in prescribing morphological features and stages of diabetic retinopathy. A new colour correction algorithm, *f*TBCSSR*hm*, is proposed to address image size uncertainty and standardise the colour of retinal fundus images. Second, to enhance the bright and dark regions of interest within standard colour retinal fundus images. A new improvised algorithm, *e*TBCSSR-HPSOCS, is proposed, a hybrid of TBCSSR and HPSOCS algorithms. The *e*TBCSSR-HPSOCS improves the β parameter using a fuzzy ruled-based model and integrates with histogram matching of standard colour retinal fundus images. The HPSOCS improves by implementing the lightness component of LAB colour space as velocity determination in PSO. Third, the performance of the eTBCSSR-HPSOCS will be evaluated, and the three algorithms (CS, TBCSSR, and HPSOCS) will be compared. The outcome shows that the *e*TBCSSR-HPSOCS and *lav*HPSOCS resultant images are naturalistic and have a colour preference similar to the original retinal fundus image. This approach has enhanced the image's visual perception while maintaining the features' readability. This approach makes it easy to identify the areas impacted by retinal disorders.

Hence, *e*TBCSSR-HPSOCS model has been shown to improve retinal fundus images to near-natural colour, but it has limitations. Some images over-illuminate in certain areas, requiring further image enhancement. The study's data is only limited to 100 retinal fundus images from primary data sources. Addressing these limitations requires further research, including developing novel colour image processing variants, hybridising with other techniques, theoretical investigations, empirical studies, and applications in diverse problem domains. Further research is needed to address these limitations and improve the model's effectiveness.

ACKNOWLEDGMENT

This research was supported by the Ministry of Higher Education (MoHE) of Malaysia through the Fundamental Research Grant Scheme

(FRGS/1/2019/ICT02/UUM/02/1). The authors are also grateful to Professor Datin Dr. Zunaina Embong, an ophthalmologist from Hospital Universiti Sains Malaysia (HUSM), for her cooperation and knowledge sharing throughout the study. The content of this article is solely the responsibility of the authors and does not necessarily represent the official views of the MoHE, Malaysia.

REFERENCES

Al-Ameen, Z., & Sulong, G. (2015). A new algorithm for improving the low contrast of computed tomography images using tuned brightness controlled single-scale retinex. *Wiley Online Library*, *37*(December 2014), 116–125. https://doi.org/10.1002/sca.21187

Al-amri, S. S., Kalyankar, N. V., & Khamitkar, S. D. (2010). Linear and non-linear contrast enhancement image. *Journal of Computer Science*, *10*(2), 139–143. http://paper.ijcsns.org/07_book/201002/20100222.pdf

Al-amri, S. S., Kalyankar, N. V., & Khamitkar, S. D. (2011). Contrast stretching enhancement in remote sensing image. *BIOINFO Sensor Networks*, *1*(1), 4.

Azmi, K. Z. M., Abdul Ghani, A. S., Md Yusof, Z., & Ibrahim, Z. (2019). Deep underwater image enhancement through colour cast removal and optimisation algorithm. *Imaging Science Journal*, *67*(6), 330–342. https://doi.org/10.1080/13682199.2019.1660484

Badano, A., Revie, C., Casertano, A., Cheng, W., Green, P., Kimpe, T., Krupinski, E., Sisson, C., Skrøvseth, S., & Treanor, D. (2015). Consistency and standardisation of colour in medical imaging: A consensus report. *Journal of Digital Imaging*, *28*, 41–52. https://doi.org/10.1007/s10278-014-9721-0

Barrera, J., Álvarez-bajo, O., Flores, J. J., & Coello, C. A. C. (2016). Limiting the velocity in the particle swarm optimisation algorithm. *Computación y Sistemas*, *20*(4), 635–645. https://doi.org/10.13053/CyS-20-4-2505

Batchelor, B. G. (2012). Machine vision handbook. In *Machine Vision Handbook*. https://doi.org/10.1007/978-1-84996-169-1

Bhateja, V., Nigam, M., Bhadauria, A. S., Arya, A., & Zhang, E. Y. D. (2019). Human visual system based optimised mathematical morphology approach for enhancement of brain MR images. *Journal of Ambient Intelligence and Humanized Computing*, *0123456789*. https://doi.org/10.1007/s12652-019-01386-z

Bhatia, N., & Kumar Rawat, T. (2018). An improved technique for image contrast enhancement using wavelet transforms. *Proceedings of the 2017 International Conference On Smart Technology for Smart Nation, SmartTechCon 2017*, 815–819. https://doi.org/10.1109/SmartTechCon.2017.8358486

Burke, E. K., & Kendall, G. (2014). *Search methodologies: Introductory tutorials in optimisation and decision support techniques* (Second). Springer Science+Business Media Singapore.

Cai, S., Lu, Y., Li, B., Gao, Q., Xu, L., Hu, X., & Zhang, L. (2023). Segmentation of cardiac tissues and organs for CCTA images based on a deep learning model. *Frontiers in Physics*, *11*(August), 1–12. https://doi.org/10.3389/fphy.2023.1266500

Cam, H. B., Akcakoca, S., Elbir, A., Ilhan, H. O., & Aydin, N. (2018). The performance evaluation of the Cat and Particle Swarm Optimisation Techniques in the image enhancement. *2018 Electric Electronics, Computer Science, Biomedical Engineerings' Meeting, EBBT 2018*, 1–4. https://doi.org/10.1109/EBBT.2018.8391430

Cao, L., & Li, H. (2020). Enhancement of blurry retinal image based on non-uniform contrast stretching and intensity transfer. *Medical and Biological Engineering and Computing*, *58*(3), 483–496. https://doi.org/10.1007/s11517-019-02106-7

Chandrashekar, L., & Sreedevi, A. (2020). A multi-objective enhancement technique for poor contrast magnetic resonance images of brain glioblastomas. *Procedia Computer Science*, *171*(2019), 1770–1779. https://doi.org/10.1016/j.procs.2020.04.190

Chew, F. L. M., Salowi, M. A., Mustari, Z., Husni, M. A., Hussein, E., Adnan, T. H., Ngah, N. F., Limburg, H., & Goh, P. P. (2018). Estimates of visual impairment and its causes from the national eye survey in Malaysia (NESII). *PLoS ONE*, *13*(6), 1–11. https://doi.org/10.1371/journal.pone.0198799

Colomer, A., Igual, J., & Naranjo, V. (2020). Detection of early signs of diabetic retinopathy based on textural and morphological information in fundus images. *Sensors (Switzerland)*, *20*(4). https://doi.org/10.3390/s20041005

Dabass, J., & Vig, R. (2018). Biomedical image enhancement using different techniques - A comparative study. *Communications in Computer and Information Science*, *799*, 260–286. https://doi.org/10.1007/978-981-10-8527-7_22

Deepak, P. R., Neelamegam, P., Sriram, S., & Nagarajan, R. (2012). Enhancement of vein patterns in hand image for biometric and biomedical application using various image enhancement techniques. *Procedia Engineering*, *38*, 1174–1185. https://doi.org/10.1016/j.proeng.2012.06.149

DeMarco, H. W., Mah, D., Cole, J., & Mazzarella, J. (2018). Busted barriers: Triaging retinal hemorrhages. *9th Annual Retina Report*.

Deshpande, A. R., & Emmanuel, M. (2016). Recent advances in colour object recognition: A review. In *Signal Processing and Computer Vision* (Issue November 2018, pp. 447–455). Excel Academy Publishers.

Elloumi, Y., Akil, M., & Boudegga, H. (2019). Ocular diseases diagnosis in fundus images using a deep learning: Approaches, tools and performance evaluation. *Real-Time Image Processing and Deep Learning 2019*, *33*(0), 30. https://doi.org/10.1117/12.2519098

Fang, F. (2021). *Integrating colour correction algorithms*. *December*. https://ueaeprints.uea.ac.uk/id/eprint/83519/%0Ahttps://ueaeprints.uea.ac.uk/id/eprint/83519/1/2021FangFPhD.pdf

Fathy, W. E., Ghoneim, A. S., Zarif, S., & Youssif, A. A. (2018). Benchmarking of pre-processing methods employed in facial image analysis. *Journal of Image and Graphics*, *6*(1), 1–9. https://doi.org/10.18178/joig.6.1.1-9

Faridul H.S., Pouli T., Chamaret C., Stauder J., E Reinhard., Kuzovkin D., Tremeau A. (2016). Colour mapping: A review of recent methods, extensions and applications. *Computer Graphics Forum, 35*(1), 59-88. https://doi.org/10.1111/cgf.12671

Garcia-Lamont, F., Cervantes, J., López, A., & Rodriguez, L. (2018). Segmentation of images by colour features: A survey. *Neurocomputing*, *292*, 1–27. https://doi.org/10.1016/j.neucom.2018.01.091

Gonzalez, R. C., & Woods, R. E. (2008). Histogram Equalization. In *Digital Image Processing* (Third Edit, pp. 1–8).

Gonzalez, R. C., & Woods, R. E. (2017). *Digital Image Processing* (4th edition). Pearson Education (US).

Grundland, M., & Dodgson, N. A. (2007). Decolorize: Fast, contrast enhancing, color to grayscale conversion. *Pattern Recognition*, *40*(11), 2891-2896.

Gu, Z., Chen, C., & Zhang, D. (2018). A low-light image enhancement method based on image degradation model and pure pixel ratio

prior. *Mathematical Problems in Engineering*, *2018*, 19. https://doi.org/10.1155/2018/8178109

Guo, X.-X. (2020). Measurements of the parapapillary atrophy area and other fundus morphological features in high myopia with or without posterior staphyloma and myopic traction maculopathy. *International Journal of Ophthalmology*, *13*(8), 1272–1280. https://doi.org/10.18240/ijo.2020.08.14

Harun, N. H., Bakar, J. A., Wahab, Z. A., Osman, M. K., & Harun, H. (2020). Colour image enhancement of acute leukemia cells in blood microscopic image for leukemia detection sample. *ISCAIE 2020 - IEEE 10th Symposium on Computer Applications and Industrial Electronics*, *3*, 24–29. https://doi.org/10.1109/ISCAIE47305.2020.9108810

Hegde, R. B., Prasad, K., Hebbar, H., & Singh, B. M. K. (2019). Comparison of traditional image processing and deep learning approaches for classification of white blood cells in peripheral blood smear images. *Biocybernetics and Biomedical Engineering*, *39*(2), 382–392. https://doi.org/10.1016/j.bbe.2019.01.005

Huang Y., Lin L., Li M., Wu J., Cheng P., Wang K., Yuan J., Tang X. (2020). Automated hemorrhage detection from coarsely annotated fundus images in diabetic retinopathy. *2020 IEEE 17th International Symposium on Biomedical Imaging (ISBI),* Iowa City, IA, USA, 2020, 1369-1372, https://doi.org/10.1109/ISBI45749.2020.9098319.

Hussein, R. R., Hamodi, Y. I., & Sabri, R. A. (2019). Retinex theory for colour image enhancement: A systematic review. *International Journal of Electrical and Computer Engineering*, *9*(6), 5560–5569. https://doi.org/10.11591/ijece.v9i6.pp5560-5569

Ibraheem, N. A, Hasan, M. M., Khan, R. Z., & Mishra, P. K. (2012). Understanding colour models: A review. *ARPN Journal of Science and Technology*, *2*(3), 265–275.

Jyotismita Chaki, N. D. (2021). Introduction to Image Colour Feature. *SpringerBriefs in Applied Sciences and Technology*. https://doi.org/https://doi.org/10.1007/978-981-15-5761-3_1

Kagarlitsky, S., Moses, Y., & Hel-Or, Y. (2009). Piecewise-consistent colour mappings of images acquired under various conditions. *Proceedings of the IEEE International Conference on Computer Vision*, 2311–2318. https://doi.org/10.1109/ICCV.2009.5459437

Kaur, J., & Choudhary, A. (2012). Comparison of several contrast stretching techniques on acute leukemia images. *International Journal of Engineering and Innovative Technology*, *2*(1), 332–335.

Kendall, D. G. (1984). Shape manifolds, procrustean metrics, and complex projective spaces. *Bulletin of the London Mathematical Society*, *16*(2), 81–121. https://doi.org/10.1112/blms/16.2.81

Kim, M., Yan, C., Yang, D., Wang, Q., Ma, J., & Wu, G. (2020). Deep learning in biomedical image analysis. In *Biomedical Information Technology* (Second Edi). Elsevier. https://doi.org/10.1016/b978-0-12-816034-3.00008-0

Kumar, A., & Prateek, M. (2020). Localisation of nuclei in breast cancer using whole slide imaging system supported by morphological features and shape formulas. *Cancer Management and Research*, *12*, 4573–4583. https://doi.org/10.2147/CMAR.S248166

Kumar Vishwakarma, A., & Mishra, A. (2012). Colour image enhancement techniques: A critical review. *Indian Journal of Computer Science and Engineering (IJCSE)*, *3*(1), 39–45.

Land, E. H. (1964). The Retinex. *American Scientist*, *52*(2), 247–253, 255–264. https://doi.org/10.1002/9780470719404.ch11

Larici, A. R., Farchione, A., Franchi, P., Ciliberto, M., Cicchetti, G., Calandriello, L., del Ciello, A., & Bonomo, L. (2017). Lung nodules: Size still matters. *European Respiratory Review*, *26*(146). https://doi.org/10.1183/16000617.0025-2017

Li, J., Ren, B., & Wang, C. (2007). A random velocity boundary condition for robust particle swarm optimisation. In *Bio-Inspired Computational Intelligence and Applications: International Conference on Life System Modeling and Simulation, LSMS 2007, Shanghai, China, September 14-17, 2007. Proceedings* (pp. 92-99). Springer Berlin Heidelberg. https://doi.org/10.1007/978-3-540-74769-7_11

Lin, H., Hu, Y., Chen, S., Yao, J., & Zhang, L. (2019). Fine-grained classification of cervical cells using morphological and appearance based convolutional neural networks. *IEEE Access*, *7*, 71541–71549. https://doi.org/10.1109/ACCESS.2019.2919390

Linda G. Shapiro, G. C. S. (2001). *Computer Vision*. Upper Saddle River: Prentice–Hall.

Long, S., Chen, J., Hu, A., Liu, H., Chen, Z., & Zheng, D. (2020). Microaneurysms detection in colour fundus images using machine learning based on directional local contrast. *BioMedical Engineering Online*, *19*(1), 1–23. https://doi.org/10.1186/s12938-020-00766-3

Magliah, S. F., Bardisi, W., Attah, M. Al, & Khorsheed, M. M. (2018). The prevalence and risk factors of diabetic retinopathy

in selected primary care centers during the 3-year screening intervals. *Journal of Family Medicine and Primary Care*, *7*(5), 975–981. https://doi.org/10.4103/jfmpc.jfmpc

Martins, J., Cardoso, J. S., & Soares, F. (2020). Offline computer-aided diagnosis for Glaucoma detection using fundus images targeted at mobile devices. *Computer Methods and Programs in Biomedicine*, *192*. https://doi.org/10.1016/j.cmpb.2020.105341

Ministry of Health Malaysia. (2015). Clinical practice guidelines: Screening for diabetic retinopathy. In *Ministry of Health Malaysia*.

Mohammed, F. G., Rada, H. M., & Mohammed, S. G. (2013). Contrast and brightness enhancement for low medical X-ray images. *International Journal of Scientific & Engineering Research, 4*(5), 1519–1523.

Mohanapriya, N., & Kalaavathi, B. (2014). Image enhancement using multilevel contrast stretching and noise smoothening technique for CT images. *International Journal of Scientific & Engineering Research, 5*(5), 713–718.

Pai, A. D. (2019). Assessment of colour normalisation algorithms under various illuminations. *International Journal of Innovative Technology and Exploring Engineering*, *8*(11), 225–228. https://doi.org/10.35940/ijitee.K1291.0981119

Panwar, N., Huang, P., Lee, J., Keane, P. A., Chuan, T. S., Richhariya, A., Teoh, S., Lim, T. H., Agrawal, R., Colomer, A., Igual, J., Naranjo, V., Sultana, R., & Rajasekhar, K. S. (2020). Diabetic retinopathy classification using haralick features. *International Journal of Recent Technology and Engineering*, *20*(4), 1323–1327. https://doi.org/10.3390/s20041005

Paul, E., Anand, R., Vivek Karthick, P., Paramasivam, M. E., & Dinesh, P. M. (2019). Image contrast enhancement using particle swarm optimisation. *Journal of Advanced Research in Dynamical and Control Systems*, *11*(4 Special issue), 1192–1196.

Paulus, D. W. R., & Hornegger, J. (1995). Intensity images. In *Pattern Recognition and Image Processing in C++* (pp. 139–140). Vieweg+Teubner Verlag. https://doi.org/https://doi.org/10.1007/978-3-322-87867-0_11

Qureshi, I., Ma, J., & Shaheed, K. (2019). A hybrid proposed fundus image enhancement framework for diabetic retinopathy. *Algorithms*, *12*(1), 1–16. https://doi.org/10.3390/a12010014

Raj, A., & Martini, M. G. (2019). *Fundus image quality assessment: Survey, challenges, and future scope. The cop*. *September*. https://doi.org/10.1049/iet-ipr.2018.6212

Rashid, R. binti A. (2023). *Types of screening for visual and eye examination*. Health Online Unit, Ministry of Health Malaysia. http://www.myhealth.gov.my/en/types-of-screening-for-visual-and-eye-examination/

Rastislav Lukac, & Plataniotis, K. N. (2011). A taxonomy of colour image filtering and enhancement solutions. In *Advance in Imaging and Electron Physics* (pp. 187–257). Elsevier.

Ratanapakorn, T., Daengphoonphol, A., Eua-Anant, N., & Yospaiboon, Y. (2019). Digital image processing software for diagnosing diabetic retinopathy from fundus photograph. *Clinical Ophthalmology*, *13*, 641–668. https://doi.org/10.2147/OPTH.S195617

Sarangi, P. P., Mishra, B. S. P., Majhi, B., & Dehuri, S. (2014). Gray-level image enhancement using differential evolution optimisation algorithm. *2014 International Conference on Signal Processing and Integrated Networks, SPIN 2014*, 95–100. https://doi.org/10.1109/spin.2014.6776929

Shapira, D., Avidan, S., & Yacov Hel-Or. (2013). Multiple histogram matching. *Proceedings of the IEEE International Conference on Image Processing*, 2269–2273.

Sharif, M., & Shah, J. H. (2019). Automatic screening of retinal lesions for grading diabetic retinopathy. *International Arab Journal of Information Technology*, *16*(4), 766–774.

Singh, N., Kaur, L., & Singh, K. (2019). Histogram equalisation techniques for enhancement of low radiance retinal images for early detection of diabetic retinopathy. *Engineering Science and Technology, an International Journal*, *22*(3), 736–745. https://doi.org/10.1016/j.jestch.2019.01.014

Solomon, S. D., Chew, E., Duh, E. J., Sobrin, L., Sun, J. K., VanderBeek, B. L., Wykoff, C. C., & Gardner, T. W. (2017). Diabetic retinopathy: A position statement by the American Diabetes Association. *Diabetes Care*, *40*(3), 412–418. https://doi.org/10.2337/dc16-2641

Sousa-ferreira, I., & Sousa, D. (2017). A review of velocity-type PSO variants. *Journal of Algorithms & Computational Technology*, *11*(1), 23–30. https://doi.org/10.1177/1748301816665021

Subramanya Jois, S. P., Harsha, S., & Harish Kumar, J. R. (2019). Automatic optic disc localisation using Particle Swarm Optimisation Technique. *IEEE Region 10 Annual International Conference, Proceedings/TENCON*, *2018* (October), 1718–1722. https://doi.org/10.1109/TENCON.2018.8650053

Swamy, J. S., & Sakkara, S. (2017). Implementation of image enhancement techniques for vein patterns in eye. *International Conference on Signal Processing, Communication, Power and Embedded System, SCOPES 2016 - Proceedings*, 390–395. https://doi.org/10.1109/SCOPES.2016.7955859

Tian, D. P. (2013). A review on image feature extraction and representation techniques. *International Journal of Multimedia and Ubiquitous Engineering*, *8*(4), 385–395.

Wei, R., Lin, K., Yan, W., Guo, Y., Wang, Y., Li, J., & Zhu, J. (2019). Computer-aided diagnosis of pancreas serous cystic neoplasms: A radiomics method on preoperative MDCT images. *Technology in Cancer Research and Treatment*, *18*(12), 1–9. https://doi.org/10.1177/1533033818824339

Xiao, B., Tang, H., Jiang, Y., Li, W., & Wang, G. (2018). Brightness and contrast controllable image enhancement based on histogram specification. *Neurocomputing*, *275*, 2798–2809. https://doi.org/10.1016/j.neucom.2017.11.057

Yadav, S. K., Kumar, S., Kumar, B., & Gupta, R. (2017). Comparative analysis of fundus image enhancement in detection of diabetic retinopathy. *IEEE Region 10 Humanitarian Technology Conference 2016, R10-HTC 2016 - Proceedings*. https://doi.org/10.1109/R10-HTC.2016.7906814

Yasui, Y., Hannon, C. P., Fraser, E. J., Ackermann, J., Boakye, L., Ross, K. A., Duke, G. L., Shimozono, Y., & Kennedy, J. G. (2019). Lesion size measured on MRI does not accurately reflect arthroscopic measurement in talar osteochondral lesions. *Orthopaedic Journal of Sports Medicine*, *7*(2), 8–12. https://doi.org/10.1177/2325967118825261